Title

HIGH TEMPERATURE THERMODYNAMIC PROPERTIES OF AQUEOUS SODIUM SULFATE SOLUTIONS

Authors

Rogers, P.S.Z.
Pitzer, K.S.

Publication Date

1981-03-01

LBL-12415
Preprint

Lawrence Berkeley Laboratory
UNIVERSITY OF CALIFORNIA, BERKELEY

EARTH SCIENCES DIVISION

Submitted to the Journal of Physical Chemistry

HIGH TEMPERATURE THERMODYNAMIC PROPERTIES OF AQUEOUS SODIUM SULFATE SOLUTIONS

P.S.Z. Rogers and Kenneth S. Pitzer

March 1981

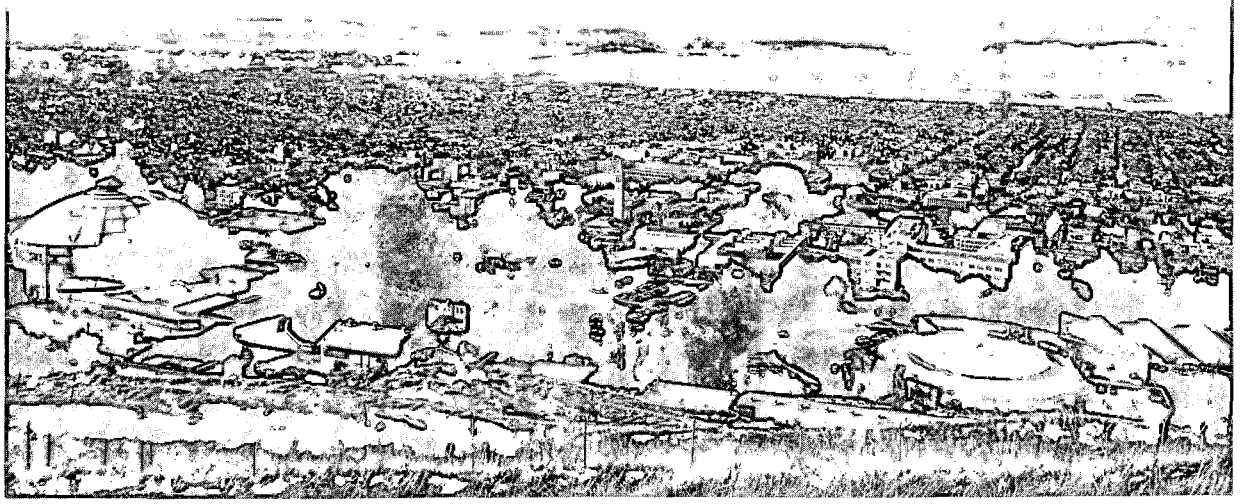

Prepared for the U.S. Department of Energy under Contract W-7405-ENG-48

DISCLAIMER

HIGH TEMPERATURE THERMODYNAMIC PROPERTIES OF AQUEOUS SODIUM SULFATE SOLUTIONS

P. S. Z. Rogers and Kenneth S. Pitzer

University of California and Lawrence Berkeley Laboratory
Berkeley, California 94720

(abstract)

A flow calorimeter has been used to measure the heat capacities of aqueous sodium sulfate solutions from 30°C to 200°C at 1 bar, or the saturated vapor pressure, and at 200 bar. The heat capacity data have been integrated as a function of temperature to obtain values of the apparent molal enthalpy, osmotic coefficient, and mean activity coefficient. Osmotic coefficients obtained in this manner are in good agreement with available literature data over the entire temperature range. These results indicate that heat capacity measurements can be used reliably to obtain the high temperature activity properties of electrolyte solutions, provided the enthalpy and Gibbs energy are known at 25°C.

This work was supported by the Director, Office of Energy Research, Office of Basic Energy Sciences of the U.S. Department of Energy under Contract No. W-7405-ENG-48.

Introduction

The thermodynamic properties of electrolyte solutions have been studied extensively at room temperature and pressure. However, comparatively little is known about the behavior of aqueous electrolytes at higher temperatures and pressures. While sodium chloride solutions have been studied at high temperatures, much less information is available on electrolytes of charge type other than 1-1. We have determined the high temperature thermodynamic properties of aqueous sodium sulfate because it provides an example of a higher charge type salt.

The thermodynamic properties of aqueous solutions are of interest for research and engineering design in such areas as desalination, geothermal energy development, geopressurized brine exploration, and hydrothermal ore deposition. The number of electrolyte solutions of interest at high temperatures is large, so that a method of obtaining thermodynamic properties from a minimum amount of experimental data is desirable. Heat capacity measurements are ideal for this purpose, since the data can be integrated to yield enthalpy and activity information, using literature data available at room temperature to evaluate the integration constants.

We have constructed a flow calorimeter to measure the heat capacities of aqueous solutions at high temperatures and pressures. Sodium chloride, the most abundant component of natural brines, has been studied previously by a number of investigators.[1-3] Sodium sulfate was chosen for this study because it is also a major component of natural brines. In addition, osmotic coefficients for sodium sulfate solutions, derived from the heat capacity measurements, can be compared with isopiestic data available at high temperatures. Sodium sulfate also is of interest in studies of ion-pair formation at elevated temperatures and as an example of a 2-1 charge-type salt.

Experimental

Flow calorimetry has many features which make it ideal for use at high temperature. Since the experimental fluid flows through the calorimeter, it is possible to keep the calorimeter temperature constant while changing samples. There is no vapor phase; hence no corrections for vaporization. Fluid flowing through the calorimeter can also be kept at constant pressure, allowing measurements along isobars rather than along the saturated vapor pressure curve. The capability to extend measurements to high pressures is limited only by the fluid pump and the back pressure regulation system. The fast response and high sensitivity which make flow calorimetry powerful at room temperature also are advantageous at high temperatures.

The high temperature, flow calorimeter is an adaptation of a design used by Picker, Leduc, Philip, and Desnoyers[4] at room temperature. It has been described in detail elsewhere;[5] in addition, Smith-Magowan and Wood[3] have constructed a similar flow calorimeter for use at high temperatures. The calorimeter is constructed of small, thin-walled tubing supported inside a large copper shield, as shown in Figure 1. Using a high pressure liquid chromatography pump, solution is forced through the tubing and past a heater, which is wound around the outside of the tubing. The solution is heated by $\sim$3K, and this temperature rise is detected by a platinum resistance thermometer contained in a spiral of the tubing. A second, identical unit of the calorimeter contains pure water flowing in series with the solution. In practice, only pure water is fed through the chromatography pump and the reference side of the calorimeter. The water then displaces an equal volume of solution, contained in a sample exchange loop thermostated at 25°C, through the working side of the calorimeter.

When water is flowing through the reference side of the calorimeter and solution is flowing through the working side, the power to the solution heater (p_s) can be adjusted until the temperature increments on both sides of the calorimeter are the same. In this case, the ratio of the specific heat capacity of the solution (c_{p_s}) to that of pure water (c_{p_w}) is given by[5]

$$\frac{c_{p_s}}{c_{p_w}} = \left(\frac{p_s - L}{p_w - L}\right)\left(\frac{\rho_w}{\rho_s}\right) \quad ,$$

where ρ_s and ρ_w are the densities of the solution and of pure water at 25°C and the system pressure. The power loss (L) is measured directly with pure water by noting the total temperature rise resulting from a known power input at a known flow rate, the heat capacity of water being known.

The solutions used in this study were prepared from Baker reagent grade anhydrous sodium sulfate, which was dried overnight at 180°C and cooled in a vacuum desiccator. All solutions were prepared by weight, and all weights were corrected for air buoyancy. At room temperature (22°C) sodium sulfate solutions are saturated at 1.56 molal.[6] Since supersaturated solutions of sodium sulfate are relatively stable, a few attempts were made to load the solution exchange loop with samples at high concentrations. These attempts were not entirely successful, and the few data points reported above 1.5 m should be used with caution.

Results

The results of heat capacity measurements of sodium sulfate solutions from 30°C to 200°C are given in Table I. The values listed for the heat capacity of pure water below 95°C were taken from Stinson,[7] while those above 95°C were taken from the steam tables of Haar, Gallagher, and Kell.[8]

The density of water at 25°C was taken as 0.997047 g cm^{-3} at 1 bar and as 1.0059 g cm^{-3} at 200 bar.[8] Densities of sodium sulfate solutions at 25°C and 1 bar were taken from the literature.[9-12] Those at 200 bar were taken from Chen, Emmet, and Millero[13] below .33 molal; above .33 molal they were estimated from values of the bulk compressibility to 1000 bar.[14] Heat capacity data along the vapor saturation curve were analyzed by assuming that the ratio (ρ_s/ρ_w) at 25°C does not vary over the small pressure range from 1 bar to 16 bar.

Likke and Bromley[15] have published the only comprehensive study of the heat capacities of sodium sulfate solutions at high temperatures. Their data are compared with that of the present study in Figure 2, where the error bars shown for the 180°C data were calculated using the uncertainty of ± .01 Jg^{-1} K^{-1} (in the specific heat capacity) given by Likke and Bromley. The two sets of data are in agreement well within the stated uncertainty. However, the greater precision of the present measurements is evident at the lower concentrations. No literature data on sodium sulfate heat capacities are available at pressures greater than the saturated vapor pressure. The 200 bar data at 50°C and 140°C are compared with low pressure data in Figures 3 and 4. The pressure dependence of the apparent molal heat capacity of Na_2SO_4 at 50°C is twice as large as that reported by Smith-Magowan and Wood[3] for NaCl.

Calculations

Review of Equations. To calculate high temperature activity properties, the heat capacity data must be fit to a temperature dependent equation, and the fitting equation must be integrated twice using enthalpy and activity data at 25°C to evaluate the integration constants. The system of

Table I

The Heat Capacity of Aqueous Sodium Sulfate

T = 304.62 K (31.47°C)

molality	$\left(\frac{c_{p_s}}{c_{p_w}}\right)_T$	$\left(\frac{\rho_s}{\rho_w}\right)_{25°C}$	ρ_s(25°C)(g/cm^3)	c_{p_s} (Jg^{-1}K^{-1})	ϕ_{C_p}(Jmol^{-1}K^{-1})
	P = 1.01 bar	P = 1.01 bar	P = 1.01 bar	P = 1.01 bar	P = 1.01 bar
0	1.0000	.997047	4.1780	-	
.0528	.9978	1.0038	4.1408	-116.	
.0528	.9977	1.0038	4.1403	-126.	
.0995	.9960	1.0097	4.1092	-108.	
.2491	.9917	1.0279	4.0188	- 68.3	
.4986	.9884	1.0572	3.8946	- 15.2	
.7486	.9878	1.0853	3.7913	22.0	
.9995	.9891	1.1125	3.7036	51.4	
1.9407	.9939	1.2060	3.4329	103.7	

T = 324.00 K (50.85°C)

molality	$\left(\frac{c_{p_s}}{c_{p_w}}\right)_T$	$\left(\frac{\rho_s}{\rho_w}\right)_{25°C}$	ρ_s(25°C)(g/cm^3)	c_{p_s} (Jg^{-1}K^{-1})	ϕ_{C_p}(Jmol^{-1}K^{-1})
	P = 1.01 bar	P = 1.01 bar	P = 1.01 bar	P = 1.01 bar	P = 1.01 bar
0	1.0000	.997047	4.1807	-	
.0500	.9980	1.0034	4.1457	-111.	
.1092	.9966	1.0109	4.1095	- 68.3	
.2832	.9935	1.0320	4.0128	- 22.9	
.2832	.9937	1.0320	4.0137	- 19.6	
.4995	.9911	1.0573	3.9073	7.6	
.4995	.9916	1.0573	3.9093	11.9	
.7487	.9910	1.0854	3.8058	39.8	
1.0089	.9921	1.1135	3.7139	64.8	
1.4430	.9967	1.1581	3.5873	98.3	
2.0394	1.0064	1.2152	3.4522	133.1	

Table I (continued)

T = 349.18 K (76.03°C)

molality	$\left(\frac{c_{p_s}}{c_{p_w}}\right)_T \left(\frac{\rho_s}{\rho_w}\right)_{25°C}$	ρ_s(25°C)(g/cm^3)	c_{p_s} (Jg^{-1}K^{-1})	ϕ_{C_p}(Jmol^{-1}K^{-1})
	P = 1.01 bar	P = 1.01 bar	P = 1.01 bar	P = 1.01 bar
0	1.0000	.997047	4.1932	-
.0500	.9984	1.0034	4.1600	- 73.
.1092	.9970	1.0109	4.1233	- 54.
.2832	.9944	1.0320	4.0285	- 9.4
.4995	.9927	1.0573	3.9254	21.4
.7487	.9920	1.0854	3.8211	45.8
1.0089	.9929	1.1135	3.7280	68.4
1.4430	.9974	1.1581	3.6006	100.8
2.0394	.9947	1.2152	3.4222	108.0

T = 413.90 K (140.75°C)

molality	$\left(\frac{c_{p_s}}{c_{p_w}}\right)_T \left(\frac{\rho_s}{\rho_w}\right)_{25°C}$	ρ_s(25°C)(g/cm^3)	c_{p_s} (Jg^{-1}K^{-1})	ϕ_{C_p}(Jmol^{-1}K^{-1})
	P = 5 bar	P = 3.69 bar	P = 3.69 bar	P = 3.69 bar
0	1.0000	.997047	4.2901	-
.0528	.9976	1.0038	4.2510	-137.
.0995	.9961	1.0097	4.2200	-105.
.2491	.9922	1.0279	4.1288	- 61.1
.4986	.9874	1.0572	3.9950	- 24.4
.7486	.9850	1.0853	3.8820	6.3
.9995	.9834	1.1125	3.7810	27.7
1.9407	.9841	1.2060	3.4903	83.6
2.6294	.9936	1.2673	3.3537	120.2

Table I (continued)

T = 450.41 K (177.26°C)

molality	$\left(\frac{c_{p_s}}{c_{p_w}}\right)_T \left(\frac{\rho_s}{\rho_w}\right)_{25°C}$	ρ_s(25°C)(gm/cm^3)	c_{p_s} (Jg^{-1}K^{-1})	ϕ_{C_p} (Jmol^{-1}K^{-1})
	P = 10 bar	P = 9.40 bar	P = 9.40 bar	P = 9.40 bar
0	1.0000	.997047	4.3934	-
.0528	.9967	1.0038	4.3494	-215.
.0995	.9940	1.0097	4.3123	-203.
.2491	.9883	1.0279	4.2117	-131.
.4986	.9814	1.0572	4.0664	- 78.2
.7486	.9766	1.0853	3.9417	- 43.5
.9995	.9731	1.1125	3.8315	- 17.9
1.9407	.9677	1.2060	3.5149	46.6

T = 474.68 K (201.53°C)

molality	$\left(\frac{c_{p_s}}{c_{p_w}}\right)_T \left(\frac{\rho_s}{\rho_w}\right)_{25°C}$	ρ_s(25°C)(gm/cm^3)	c_{p_s} (Jg^{-1}K^{-1})	ϕ_{C_p} (Jmol^{-1}K^{-1})
	P = 17 bar	P = 16.04 bar	P = 16.04 bar	P = 16.04 bar
0	1.0000	.997047	4.4966	-
.0528	.9952	1.0038	4.4449	-348.
.0995	.9922	1.0097	4.4056	-289.
.2491	.9848	1.0279	4.2953	-198.

Table I (continued)

T = 323.81 K (50.66°C)

molality	$\left(\frac{c_{p_s}}{c_{p_w}}\right)_T \left(\frac{\rho_s}{\rho_w}\right)_{25°C}$	ρ_s(25°C)(g/cm^3)	c_{p_s} (Jg^{-1}K^{-1})	$^{\phi}C_p$(Jmol^{-1}K^{-1})
	P = 207.2 bar	P = 200 bar	P = 200 bar	P = 200 bar
0	1.0000	1.0059	4.1379	-
.0528	.9985	1.0126	4.1044	- 51.
.0528	.9985	1.0126	4.1044	- 51.
.0995	.9975	1.0184	4.0769	- 34.
.0995	.9973	1.0184	4.0761	- 42.
.2491	.9948	1.0362	3.9960	- 2.0
.2491	.9946	1.0362	3.9952	- 5.4
.4986	.9929	1.0650	3.8805	34.9
.7486	.9931	1.0928	3.7826	62.7
.9995	.9946	1.1196	3.6976	84.7
1.9407	.9907	1.2121	3.4020	104.0
2.6294	.9756	-	-	-

T = 414.20 K (131.05°C)

molality	$\left(\frac{c_{p_s}}{c_{p_w}}\right)_T \left(\frac{\rho_s}{\rho_w}\right)_{25°C}$	ρ_s(25°C)(g/cm^3)	c_{p_s} (Jg^{-1}K^{-1})	$^{\phi}C_p$(Jmol^{-1}K^{-1})
	P = 199.2 bar	P = 200 bar	P = 200 bar	P = 200 bar
0	1.0000	1.0059	4.2363	-
.0528	.9978	1.0126	4.1991	-108.
.0995	.9963	1.0184	4.1689	- 85.
.2491	.9927	1.0362	4.0824	- 38.0
.4986	.9889	1.0650	3.9568	1.5
.7486	.9866	1.0928	3.8472	26.7
.9995	.9855	1.1196	3.7509	47.1
1.9407	.9869	1.2121	3.4696	97.8
2.6294	.9913	-	-	-

equations chosen to complete this calculation for sodium sulfate solutions was developed by Pitzer and co-workers[16-19] and was found to describe successfully the properties of sodium chloride solutions at high temperatures.[1,2] The basic equations for the osmotic and activity coefficients (ϕ and $\gamma_{\pm}$), the apparent molal enthalpy ($^{\phi}L$), and the apparent molal heat capacity ($^{\phi}C_p$) have been derived by Pitzer[20] and are summarized in Table II. Here $\beta^{(0)}$, $\beta^{(1)}$, and C^{ϕ} are the virial coefficients related to short range interionic forces whose temperature dependence will be determined from the heat capacity data. Also, the additional symbols $\beta^{(0)L}$ and $\beta^{(0)J}$ are defined as

$$\beta^{(0)L} = \left(\frac{\partial \beta^{(0)}}{\partial T}\right)_P \tag{14a}$$

$$\beta^{(0)J} = \left(\frac{\partial \beta^{(0)L}}{\partial T}\right)_P + \frac{2}{T}\beta^{(0)L} \tag{14b}$$

with similar definitions for $\beta^{(1)L}$, $C^{\phi L}$, $\beta^{(1)J}$, and $C^{\phi J}$. Values of the Debye-Hückel slopes have been calculated using the equation for the dielectric constant of pure water (D) given by Bradley and Pitzer[21] and values for the density of pure water (d_w) given by Haar, et. al.[8]

Use of eq. 8 to describe the low pressure sodium sulfate heat capacities as a function of temperature requires one approximation. The definitions of $\beta^{(0)J}$ and the other parameters require temperature derivatives at constant pressure. However, the heat capacity data have been taken along the saturated vapor pressure curve, so that above 100°C the required first derivative of $\beta^{(0)}$ is

$$\left(\frac{\partial \beta^{(0)}}{\partial T}\right)_P = \left(\frac{\alpha \beta^{(0)}}{\partial T}\right)_{sat} - \left(\frac{\partial \beta^{(0)}}{\partial P}\right)_T \left(\frac{\partial P}{\partial T}\right)_{sat} . \tag{15}$$

Table II

Pitzer's Equations for the Thermodynamic Properties of an Aqueous Electrolyte Solution

Osmotic Coefficient

$$\phi - 1 = -|Z_M Z_X| A_\phi \frac{I^{1/2}}{1+1.2I^{1/2}} + \left(\frac{2\nu_M\nu_X}{\nu}\right)m B^\phi_{MX} + \left(\frac{2(\nu_M\nu_X)^{3/2}}{\nu}\right)m^2 C^\phi_{MX} \quad (1)$$

$$B^\phi_{MX} = \beta^{(0)}_{MX} + \beta^{(1)}_{MX} e^{-\alpha I^{1/2}} \quad (2)$$

Activity Coefficient

$$\ln \gamma\pm = -|Z_M Z_X| A_\phi \left[\frac{I^{1/2}}{1+1.2I^{1/2}} + \frac{2}{1.2}\ln(1+1.2I^{1/2})\right] + \left(\frac{2\nu_M\nu_X}{\nu}\right)m B^\gamma_{MX} + \left(\frac{3(\nu_M\nu_X)^{3/2}}{\nu}\right)m^2 C^\phi_{MX} \quad (3)$$

$$B^\gamma_{MX} = 2\beta^{(0)}_{MX} + \frac{2\beta^{(1)}_{MX}}{\alpha^2 I}\left[1 - \left(1+\alpha I^{1/2} - \frac{\alpha^2 I}{2}\right) e^{-\alpha I^{1/2}}\right] \quad (4)$$

Apparent Molal Enthalpy

$$\phi_L = \nu|Z_M Z_X| A_H \frac{\ln(1+1.2I^{1/2})}{2.4} - 2\nu_M\nu_X RT^2 \left[m B^L_{MX} + m^2(\nu_M Z_M) C^L_{MX}\right] \quad (5)$$

$$B^L_{MX} = \left(\frac{\partial\beta^{(0)}_{MX}}{\partial T}\right)_p + \left(\frac{\partial\beta^{(1)}_{MX}}{\partial T}\right)_p \left(\frac{2}{\alpha^2 I}\right)\left[1 - \left(1+\alpha I^{1/2}\right) e^{-\alpha I^{1/2}}\right] \quad (6)$$

$$C^L_{MX} = \left(\frac{1}{2|Z_M Z_X|^{1/2}}\right)\left(\frac{\partial C^\phi_{MX}}{\partial T}\right)_p \quad (7)$$

Table II (continued)

Apparent Molal Heat Capacity

$$\phi C_p = \overline{C_{p_2}}^{\circ} + \nu|Z_M Z_X| A_J \frac{\ln(1+1.2I^{\frac{1}{2}})}{2.4} - 2\nu_M\nu_X RT^2[m B_{MX} + m^2(\nu_M Z_M) C^J_{MX}] \quad (8)$$

$$B^J_{MX} = \left(\frac{\partial \beta^L_{MX}}{\partial T}\right)_{P,I} + \frac{2}{T} B^L_{MX} \quad (9)$$

$$C_{MX} = \left(\frac{\partial C^L_{MX}}{\partial T}\right)_P + \frac{2}{T} C^L_{MX} \quad (10)$$

Debye-Hückel Slopes

$$A_\phi = (1/3)(2\pi N_o d_w/1000)^{\frac{1}{2}} (e^2/DkT)^{3/2} \quad (11)$$

$$A_H = 4RT^2(\partial A_\phi/\partial T)_P \quad (12)$$

$$A_J = (\partial A_H/\partial T)_P \quad (13)$$

Definitions of Symbols

α a constant with value 2.0

$\beta^{(0)}_{MX}$, $\beta^{(1)}_{MX}$, C^{ϕ}_{MX} fitting parameters

m molality of the solute

I ionic strength ($\frac{1}{2} \sum_i m_i Z_i^2$)

ν total number of ions formed from dissociation of salt MX ($\nu = \nu_M + \nu_X$)

Z_M, Z_X charges on ions M and X

$\overline{C_{p_2}}^{\circ}$ apparent molal heat capacity of the solute at infinite dilution

Extensive volumetric data at high temperatures and pressures are required to evaluate the last term in eq. 15; in this study, it has been assumed to be negligibly small. This assumption is probably reasonable below 200°C, but it could lead to significant error at higher temperatures.

Temperature Dependence of the Heat Capacity. The low pressure heat capacity data were first fit to eq. 8 at constant temperature to evaluate $\overline{C}_{p_2}^{\circ}$. These values of $\overline{C}_{p_2}^{\circ}$ were combined with those reported by Gardner, Jekel, and Cobble[22] in a least squares fitting routine to determine their temperature dependence. The two sets of $\overline{C}_{p_2}^{\circ}$ values and the smooth curve given by the fitting equation,

$$\overline{C}_{p_2}^{\circ} = U_1 + U_2T + U_3T^2 + \frac{U_4}{(T-263)} \quad , \tag{16}$$

are shown in Figure 5. The coefficients of eq. 16 are given in Table III. The values of $\overline{C}_{p_2}^{\circ}$ were fixed by this equation for the rest of the calculations.

Values of ${}^{\phi}C_p - \overline{C}_{p_2}^{\circ}$ at all temperatures, including literature data at 25°C,[9,10,23] were then used simultaneously in a linear least squares routine to determine the optimum temperature dependent equations for $\beta^{(0)J}$, $\beta^{(1)J}$, and $C^{\phi J}$:

$$\beta^{(0)J} = 6U_5 + \frac{2U_6}{T} + \frac{U_7}{T^2} + \frac{526U_8}{T(T-263)^3} \tag{17}$$

$$\beta^{(1)J} = 6U_9 + \frac{2U_{10}}{T} + \frac{U_{11}}{T^2} + \frac{526U_{12}}{T(T-263)^3} + \frac{1360U_{13}}{T(680-T)^3} \tag{18}$$

$$C^{\phi J} = \frac{2U_{14}}{T} + \frac{526U_{15}}{T(T-263)^3} \quad . \tag{19}$$

The factors $(T-263)^{-3}$ and $(680-T)^{-3}$ were chosen for convenience as factors which vary rapidly at low and high temperatures, respectively. The values

Table III

Values of the Fitting Parameters for the Heat Capacity of Na_2SO_4 as a Function of Temperature

Integration Constants at T = 298.15 K:

$\beta^{(0)} = .01869$ $\quad\quad$ $\beta^{(0)L} = .002349$

$\beta^{(1)} = 1.0994$ $\quad\quad$ $\beta^{(1)L} = .005958$

$C^{\phi} = .005549$ $\quad\quad$ $C^{\phi L} = -.00479$

Parameters for $\overline{C}_{P_2}^{\circ}$

$U_1 = -990.405$

$U_2 = 6.79636$

$U_3 = -.0117779$

$U_4 = -6518.67$

Parameters for Equations (14)-(16):

Fit of Heat Capacity and Osmotic Coefficient Data

$U_5 = -1.03611 \times 10^{-5}$ $\quad\quad$ $U_{11} = -1.88769 \times 10^{2}$

$U_6 = 3.00299 \times 10^{-2}$ $\quad\quad$ $U_{12} = -2.05974 \times 10^{-1}$

$U_7 = -1.43441 \times 10^{1}$ $\quad\quad$ $U_{13} = 1.46744 \times 10^{3}$

$U_8 = -6.66894 \times 10^{-1}$ $\quad\quad$ $U_{14} = 5.14316 \times 10^{-5}$

$U_9 = -3.23550 \times 10^{-4}$ $\quad\quad$ $U_{15} = 3.45791 \times 10^{-1}$

$U_{10} = 5.76552 \times 10^{-1}$

of 263 and 680 have no theoretical significance.

Predicted values of the osmotic coefficient were calculated from a straightforward, albeit lengthy, integration of the equations for $\beta^{(0)J}$, $\beta^{(1)J}$, and $C^{\phi J}$ to obtain $\beta^{(0)}$, $\beta^{(1)}$, and C^{ϕ}. The required integration constants are simply values of $\beta^{(0)}$, $\beta^{(1)}$, and C^{ϕ}, and their first derivatives with temperature, conveniently evaluated at 25°C. Improved values of $\beta^{(0)}$, $\beta^{(1)}$, and C^{ϕ} for sodium sulfate at 25°C have recently been calculated by Rard and Miller[24] from their isopiestic data; they are listed in Table III. The remaining integration constants were evaluated by fitting literature data available at 25°C[25-27] with eq. 5. They differ slightly from the values determined previously by Silvester and Pitzer[28] in that the value of the Debye-Hückel slope, A_H, has been improved.[21]

Osmotic coefficients calculated using the heat capacity data alone are compared with literature data[29-31] from 45°C to 120°C in Figure 6, where the osmotic coefficients predicted from this fit are shown by the solid line at low concentrations progressing to the dashed line at high concentrations. Below 100°C, the agreement of data and prediction is excellent, even to concentrations above the 1.5 molal range of the fitting equation. Since the parameters chosen as the integration constants reproduce the osmotic coefficient to high concentrations, this agreement above 1.5 m, at low temperatures, is not too surprising. These results indicate that high temperature heat capacity data, in combination with known values of the enthalpy and activity at room temperature, are sufficient to obtain accurate activity properties as a function of temperature.

The temperature dependent equations for the thermodynamic properties of sodium sulfate solutions can now be improved by including the osmotic coefficient data available below 120°C in a simultaneous fit with the heat

capacity data. This serves to extend the concentration range for activity properties calculated from the fitting equations from 1.5 to 2.5 molal. The form of the equations for $\beta^{(0)J}$, $\beta^{(1)J}$, and $C^{\phi J}$ are unchanged, and the parameters U_5 - U_{15} obtained from this combined fit are listed in Table III. (Values for the parameters obtained in the fit of the heat capacity data alone are available in Reference 5.) Osmotic coefficients calculated from the combined fit are shown by the solid line in Figure 6.

The parameters determined in the combined fit reproduce the heat capacity measurements to $\pm 3 \times 10^{-3}$ Jg^{-1} K^{-1}, in good agreement with the estimated precision of the data.[4] They can be used to calculate apparent molal heat capacities to 200°C, at concentrations up to 1.5 molal. Values of the apparent molal enthalpy can be calculated, with an estimated uncertainty of 2%, at concentrations up to 2 molal below 120°C, and to 1.5 molal above 120°C. Calculation of osmotic and activity coefficients above 120°C is limited to concentrations below 1.5 molal, because they are predicted solely from the heat capacity data. The estimated uncertainty in the calculated values for these quantities is also 2%. Calculated values of the mean activity coefficient are given in Table IV.

Discussion

Additional comparisons of thermodynamic properties calculated with the fitting equations and literature data are shown in Figures 7-9. High temperature values of the osmotic coefficient are in substantial agreement with the data of Lindsay and Liu,[35] as illustrated in Figure 7. Figure 8 shows that the predicted values of the apparent molal enthalpy are in general agreement with the data of Snipes, Manly, and Ensor[36] between 40°C and 80°C, although the difference between calculated and experimental values

TABLE IV: MEAN ACTIVITY COEFFICIENT OF AQUEOUS SODIUM SULFATE SOLUTIONS

T (°C)	P (BAR)	D-H SLOPE	MOLALITY .050	.100	.250	.500	.750	1.00	1.25	1.50	1.75	2.00	2.25	2.50
25.	1.0	3.91E-01	.536	.454	.347	.271	.231	.205	.187	.173	.163	.156	.150	.146
30.	1.0	3.95E-01	.534	.453	.347	.273	.233	.207	.190	.177	.167	.159	.153	.149
40.	1.0	4.02E-01	.530	.449	.346	.274	.235	.210	.193	.180	.171	.163	.158	.153
50.	1.0	4.10E-01	.525	.445	.343	.272	.235	.211	.194	.182	.172	.165	.159	.154
60.	1.0	4.19E-01	.519	.439	.338	.268	.232	.209	.192	.180	.171	.164	.158	.153
70.	1.0	4.28E-01	.512	.432	.331	.263	.227	.205	.189	.177	.168	.161	.155	.150
80.	1.0	4.38E-01	.504	.424	.324	.256	.221	.199	.184	.172	.164	.156	.150	.145
90.	1.0	4.49E-01	.496	.415	.315	.249	.214	.193	.178	.166	.158	.150	.144	.139
100.	1.0	4.61E-01	.486	.405	.306	.240	.206	.185	.170	.159	.150	.143	.137	.131
110.	1.4	4.73E-01	.477	.395	.296	.230	.197	.177	.162	.151	.143	.136	.129	.124
120.	2.0	4.86E-01	.466	.384	.285	.220	.188	.168	.154	.143	.135	.127	.121	.116
130.	2.7	4.99E-01	.455	.372	.273	.210	.178	.158	.145	.134				
140.	3.6	5.14E-01	.444	.360	.262	.199	.168	.149	.135	.125				
150.	4.8	5.30E-01	.432	.348	.250	.188	.158	.139	.126	.116				
160.	6.2	5.46E-01	.420	.335	.238	.177	.148	.129	.117	.107				
170.	7.9	5.63E-01	.407	.323	.225	.166	.137	.120	.108	.099				
180.	10.0	5.82E-01	.394	.309	.213	.155	.127	.110	.099	.090				
190.	12.5	6.02E-01	.381	.296	.201	.144	.117	.101	.090	.082				
200.	15.5	6.23E-01	.368	.283	.189	.134	.108	.092	.082	.074				

is in some cases as large as 8% of the calculated value. At high temperatures, predictions of the apparent molal enthalpy are in good agreement with values reported by Mayrath[37] at low concentrations. At concentrations between .5 m and 1.0 m, the values of Mayrath are substantially smaller than those obtained in the present study, as shown in Figure 9. In addition, low temperature activity coefficients calculated from the electromotive force data for sodium-amalgam electrode cells of Harned and Hecker[38] are in good agreement with the predicted values at high concentrations, but differ by as much as 2% at concentrations below .1 molal.

Some literature sources contained data that were not totally consistent with the heat capacity and osmotic coefficient data chosen for this study. High temperature osmotic coefficients obtained from the isopiestic data of Soldano and co-workers[39,40] are substantially larger than those predicted from the fit of the heat capacity data. Heat of dilution data at 50°C reported by Gritsus, Akhumov, and Zhilina[41] also are not in agreement with the predicted values. Osmotic coefficients calculated from the vapor pressure difference measurements of Fabuss and Korosi[42] behave erratically at low concentrations, indicating that the precision of the measurements is not sufficient to provide a test of the osmotic coefficient predictions.

The temperature dependences of the parameters, as determined from the combined fit, are shown in Figures 10-12. The general pattern of behavior of each of the parameters $\beta^{(0)}$, $\beta^{(1)}$, and C^{ϕ} for Na_2SO_4 is similar to that for NaCl! If substantial ion pairing were occurring, $\beta^{(0)}$ and $\beta^{(1)}$ would decrease to negative values; no such tendency is evident. The triple interaction parameter C^{ϕ} does become negative, but small, which suggests a mild tendency toward ion triplet formation. The magnitude of

this effect even at 200°C, however, is small in comparison with that for electrolytes such as $ZnCl_2$ at 25°C. Apparently, the electrostatic effects of the decrease in the dielectric constant of water with increasing temperature are well accounted for in the Debye-Hückel term since the remaining short range interactions between Na^+ and $SO_4^=$ ions, described by $\beta^{(0)}$ and $\beta^{(1)}$, remain small.

Conclusion

The quality of the heat capacity data obtained in this study and their agreement with literature data indicate that flow calorimetry is a valuable technique for high temperature studies. The successful prediction of osmotic coefficients from a temperature dependent fit of the heat capacity data shows that heat capacity measurements can be used reliably to obtain activity properties of electrolyte solutions at high temperatures.

One limitation to the use of flow calorimetry at high pressures should be mentioned. Reduction of the flow measurements to obtain specific heat capacities requires density data at room temperature and the system pressure. High pressure volumetric data, even at room temperature, are available for only a few electrolyte solutions over a very limited concentration range. In addition, integration of high pressure heat capacity data to obtain activity properties requires enthalpy and activity data at the same pressure to evaluate the integration constants. These are most easily obtained using density and expansivity data, as a function of pressure, to adjust activity and enthalpy data at one bar to the higher pressure. Thus a full treatment of flow calorimetry data requires volumetric properties, as a function of pressure, over a small temperature range. It is hoped that current interest in high pressure flow calorimetry will encourage further work in the determination of these important volumetric properties.

Acknowledgment

We thank Professor R. H. Wood for sharing his results in advance of publication and for valuable discussions. This work was supported by the Director, Office of Energy Research, Office of Basic Energy Sciences, of the U.S. Department of Energy under Contract No. W-7405-ENG-48.

Supplementary Material Available: Values for the osmotic coefficient, apparent molal enthalpy, apparent molal heat capacity, and specific heat capacity are given at rounded concentrations and temperatures in Tables V - VII (4 pages). Ordering information is available on any current masthead page.

References

(1) L. F. Silvester and K. S. Pitzer, J. Phys. Chem. 8, 1882 (1977).

(2) K. S. Pitzer, D. J. Bradley, P. S. Z. Rogers, and J. C. Peiper, Lawrence Berkeley Laboratory Report No. 8973 (1979).

(3) D. Smith-Magowan and R. H. Wood, submitted to J. Chem. Thermo.

(4) P. Picker, P.-A. Leduc, P. R. Philip, J. E. Desnoyers, J. Chem. Thermo. 3, 631 (1971).

(5) P. S. Z. Rogers, Doctoral Dissertation, University of California, Berkeley, California (1981).

(6) W. F. Linke, "Solubilities of Inorganic and Metal Organic Compounds," 4th ed., American Chemical Society, Washington, D. C., 1965, Vol. II.

(7) H. F. Stimson, Am. J. Phys. 23, 622 (1955).

(8) L. Haar, J. Gallagher, and G. S. Kell, Proceedings of the International Association for the Properties of Steam, September 1979.

(9) I. V. Olofosson, E. C. Jekel, and J. W. Cobble, J. Phys. Chem. 73, 2017 (1969).

(10) G. Perron, J. E. Desnoyers, F. J. Millero, Can. J. Chem. 53, 1134 (1975).

(11) R. E. Gibson, J. Phys. Chem. 31, 496 (1927).

(12) C.-T. A. Chen, J. H. Chen, and F. J. Millero, J. Chem. Eng. Data, 25, 307 (1980).

(13) C.-T. Chen, R. T. Emmet, and F. J. Millero, J. Chem. Eng. Data, 22, 201 (1977).

(14) R. E. Gibson, J. Am. Chem. Soc. 56, 4 (1933).

(15) S. Likke and L. A. Bromley, J. Chem. Eng. Data, 18, 189 (1973).

(16) K. S. Pitzer, J. Phys. Chem. 77, 268 (1973).

(17) K. S. Pitzer and G. Mayorga, J. Phys. Chem. 77, 2300 (1973).

(18) K. S. Pitzer and G. Mayorga, J. Soln. Chem. 3, 539 (1974).

(19) K. S. Pitzer and J. J. Kim, J. Am. Chem. Soc. 96, 5701 (1974).

(20) K. S. Pitzer in "Activity Coefficients in Electrolyte Solutions," R. M. Pytkowicz, ed., CRC Press, Boca Raton, Fl, 1979, Vol. I, Chapt. 7.

(21) D. J. Bradley and K. S. Pitzer, J. Phys. Chem. 83, 1599 (1979).

(22) W. L. Gardner, E. C. Jekel, and J. W. Cobble, J. Phys. Chem. 73, 2017 (1969).

(23) M. Randall and F. D. Rossini, J. Am. Chem. Soc. 51, 323 (1929).

(24) J. A. Rard and D. G. Miller, J. Chem. Eng. Data 26, 33 (1981).

(25) W. E. Wallace and A. L. Robinson, J. Am. Chem. Soc. 63, 958 (1941).

(26) E. Lange and H. Streeck, Z. Phys. Chem. Abt. 157, 1 (1931).

(27) P. T. Thompson, D. E. Smith, R. H. Wood, J. Chem. Eng. Data 19, 386 (1974).

(28) L. F. Silvester and K. S. Pitzer, J. Soln. Chem. 7, 327 (1978).

(29) K. L. Hellams, C. S. Patterson, B. H. Prentice, III, and M. J. Taylor, J. Chem. Eng. Data, 4, 323 (1965).

(30) W. T. Humphries, C. F. Kohrt, and C. S. Patterson, J. Chem. Eng. Data, 13, 327 (1968).

(31) J. T. Moore, W. T. Humphries, and C. S. Patterson, J. Chem. Eng. Data, 17, 180 (1972).

(32) C. S. Patterson, L. O. Gilpatrick, and B. A. Soldano, J. Chem. Soc. 2730 (1960).

(33) B. A. Soldano and C. S. Patterson, J. Chem. Soc. 937 (1962).

(34) Gy. Jakli, T. C. Chan, and W. A. Van Hook, J. Soln. Chem. 4, 71 (1975).

(35) C-T. Liu and W. T. Lindsay, Office of Saline Water Research and Development Progress Report No. 722, Int-OSW-RDPR-71-722 (1971).

(36) H. P. Snipes, C. Manly, and D. D. Ensor, J. Chem. Eng. Data 20, 287, (1975).

(37) J. E. Mayrath, Ph.D. Thesis, University of Delaware, Newark, DE (1980).

(38) H. S. Harned and J. C. Hecker, J. Am. Chem. Soc. 56, 650 (1934).

(39) B. A. Soldano and M. Meek, J. Chem. Soc. 4424 (1963).

(40) B. A. Soldano and P. B. Bien, J. Chem. Soc. (A), 1825 (1966).

(41) B. V. Gritsus, E. I. Akhumov, and L. P. Zhilina, Zh. Prikl. Khim., 44, 186 (1971).

(42) B. M. Fabuss and A. Korosi, Desalination 1, 139 (1966).

Figure Captions

Figure 1. High temperature flow calorimeter; A, stainless steel jacket; B, copper cylinder; C, vacuum; D, heater; E, temperature sensor; F, supporting tube containing electrical leads and vacuum connection.

Figure 2. Comparison of apparent molal heat capacity values obtained in this study with those published by Likke and Bromley.[15]

Figure 3. Comparison of apparent molal heat capacities at 1 bar and 200 bar, at 50°C.

Figure 4. Comparison of apparent molal heat capacities at 4 bar and 200 bar, at 140°C.

Figure 5. Comparison of values of the apparent molal heat capacity at infinite dilution. The solid line represents values obtained from the parameters listed in Table III. Squares represent the data of Gardner, Jekel, and Cobble,[22] and dots represent values obtained in this study.

Figure 6. Comparison of predicted values of the osmotic coefficient with literature data. Osmotic coefficients have been calculated from published isopiestic ratios[29-33] referenced to NaCl solutions using the tabulated values of ϕ_{NaCl} given by Pitzer, et al.[2]

Figure 7. Comparison of osmotic coefficients for Na_2SO_4 solutions. Solid lines represent osmotic coefficients predicted from the combined fit of heat capacity and osmotic coefficient data below 120°C. Points are the data of Liu and Lindsay[35] which were not included in the combined fit.

Figure 8. Comparison of values of the apparent molal enthalpy. Solid lines represent values predicted from the combined fit of heat capacity and osmotic coefficient data. Points are the data of Snipes, Manly, and Ensor.[36]

Figure 9. Comparison of apparent molal enthalpies at high temperatures. Solid lines represent values predicted from the combined fit of heat capacity and osmotic coefficient data. Points are the values reported by Mayrath.[37]

Figure 10. Temperature dependence of the fitting parameters $\beta^{(0)}$, $\beta^{(0)L}$, and $\beta^{(0)J}$.

Figure 11. Temperature dependence of the fitting parameters $\beta^{(1)}$, $\beta^{(1)L}$, and $\beta^{(1)J}$.

Figure 12. Temperature dependence of the fitting parameters C^{ϕ}, $C^{\phi L}$, and $C^{\phi J}$.

TABLE V: OSMOTIC COEFFICIENT OF AQUEOUS SODIUM SULFATE SOLUTIONS

T (°C)	P (BAR)	D-H SLOPE	MOLALITY .050	.100	.250	.500	.750	1.00	1.25	1.50	1.75	2.00	2.25	2.50
25.	1.0	3.91E-01	.828	.793	.739	.690	.660	.641	.629	.624	.623	.627	.633	.643
30.	1.0	3.95E-01	.828	.793	.741	.695	.666	.649	.638	.633	.633	.636	.641	.650
40.	1.0	4.02E-01	.827	.793	.744	.701	.675	.660	.651	.648	.647	.650	.654	.660
50.	1.0	4.10E-01	.825	.791	.744	.703	.680	.667	.660	.656	.656	.658	.662	.666
60.	1.0	4.19E-01	.822	.789	.742	.704	.682	.670	.664	.661	.661	.662	.664	.667
70.	1.0	4.28E-01	.818	.785	.739	.702	.681	.670	.664	.662	.661	.662	.663	.664
80.	1.0	4.38E-01	.814	.780	.734	.698	.678	.667	.662	.659	.658	.658	.658	.658
90.	1.0	4.49E-01	.810	.775	.728	.692	.673	.662	.657	.654	.653	.652	.651	.649
100.	1.0	4.61E-01	.804	.769	.721	.685	.666	.655	.650	.646	.645	.643	.641	.637
110.	1.4	4.73E-01	.799	.762	.713	.676	.657	.646	.641	.637	.635	.632	.629	.624
120.	2.0	4.86E-01	.792	.755	.704	.666	.647	.636	.630	.626	.623	.619	.615	.609
130.	2.7	4.99E-01	.786	.746	.694	.655	.635	.624	.618	.613				
140.	3.6	5.14E-01	.778	.737	.683	.643	.623	.611	.604	.599				
150.	4.8	5.30E-01	.771	.728	.672	.630	.609	.597	.589	.584				
160.	6.2	5.46E-01	.762	.718	.659	.616	.594	.581	.573	.567				
170.	7.9	5.63E-01	.754	.707	.646	.601	.578	.565	.556	.549				
180.	10.0	5.82E-01	.744	.696	.631	.585	.561	.547	.538	.531				
190.	12.5	6.02E-01	.735	.684	.617	.568	.543	.528	.518	.510				
200.	15.5	6.23E-01	.724	.671	.601	.550	.524	.508	.498	.489				

TABLE VI: APPARENT MOLAL ENTHALPY OF AQUEOUS SODIUM SULFATE SOLUTIONS (KJOULE/MOL)

T (° C)	P (BAR)	D-H SLOPE	MOLALITY .001	.005	.010	.050	.100	.250	.500	.750	1.000	1.250	1.500
25.	1.0	1.98E+03	.29	.57	.73	1.01	.94	.35	-.80	-1.89	-2.89	-3.79	-4.60
30.	1.0	2.15E+03	.32	.64	.82	1.24	1.28	.90	.01	-.88	-1.72	-2.50	-3.19
40.	1.0	2.51E+03	.38	.77	1.02	1.70	1.93	1.95	1.52	.97	.41	-.13	-.62
50.	1.0	2.90E+03	.45	.92	1.22	2.16	2.59	2.98	2.95	2.71	2.40	2.09	1.79
60.	1.0	3.33E+03	.52	1.07	1.44	2.64	3.26	4.01	4.37	4.41	4.34	4.23	4.11
70.	1.0	3.80E+03	.59	1.24	1.68	3.15	3.96	5.07	5.81	6.12	6.28	6.36	6.41
80.	1.0	4.31E+03	.67	1.42	1.93	3.69	4.70	6.18	7.29	7.87	8.24	8.51	8.72
90.	1.0	4.86E+03	.76	1.62	2.21	4.28	5.49	7.35	8.83	9.68	10.26	10.70	11.07
100.	1.0	5.47E+03	.86	1.84	2.51	4.90	6.34	8.59	10.45	11.57	12.35	12.97	13.50
110.	1.4	6.14E+03	.97	2.07	2.83	5.58	7.25	9.91	12.17	13.55	14.55	15.34	16.02
120.	2.0	6.87E+03	1.09	2.32	3.19	6.31	8.23	11.32	14.00	15.65	16.87	17.83	18.65
130.	2.7	7.68E+03	1.22	2.60	3.57	7.10	9.29	12.84	15.94	17.89	19.32	20.46	21.43
140.	3.6	8.56E+03	1.36	2.91	3.99	7.96	10.44	14.46	18.02	20.26	21.92	23.24	24.37
150.	4.8	9.54E+03	1.51	3.25	4.46	8.89	11.67	16.21	20.23	22.79	24.68	26.20	27.48
160.	6.2	1.06E+04	1.69	3.61	4.96	9.90	13.00	18.07	22.59	25.48	27.62	29.33	30.78
170.	7.9	1.18E+04	1.88	4.02	5.52	11.00	14.43	20.06	25.10	28.33	30.73	32.66	34.28
180.	10.0	1.32E+04	2.09	4.47	6.13	12.19	15.97	22.18	27.76	31.34	34.02	36.17	37.99
190.	12.5	1.47E+04	2.32	4.97	6.80	13.48	17.63	24.42	30.55	34.52	37.49	39.88	41.90
200.	15.5	1.64E+04	2.59	5.52	7.55	14.87	19.39	26.78	33.48	37.84	41.12	43.77	46.02

TABLE VII: APPARENT MOLAL HEAT CAPACITY OF AQUEOUS SODIUM SULFATE SOLUTIONS (JOULE/ MOL DEG)

T (°C)	P (BAR)	D-H SLOPE	$\bar{C}^{\circ}_{P_2}$	MOLALITY .050	.100	.250	.500	.750	1.000	1.250	1.500
25.	1.0	3.28E+01	-196.5	-150.3	-128.2	-81.8	-27.6	13.8	47.2	74.6	96.6
30.	1.0	3.43E+01	-174.8	-129.4	-108.8	-66.4	-17.8	19.2	49.6	75.0	96.3
40.	1.0	3.75E+01	-147.1	-101.4	-82.1	-43.9	-1.5	30.6	57.2	80.0	99.9
50.	1.0	4.09E+01	-132.5	-85.3	-66.3	-29.9	9.5	39.0	63.3	84.4	103.0
60.	1.0	4.46E+01	-126.3	-76.8	-57.7	-21.9	16.0	43.9	66.8	86.6	104.1
70.	1.0	4.87E+01	-126.4	-74.0	-54.3	-18.2	19.1	46.0	67.9	86.7	103.3
80.	1.0	5.32E+01	-131.5	-75.4	-54.9	-18.0	19.4	45.9	67.1	85.2	101.1
90.	1.0	5.82E+01	-140.6	-80.4	-58.9	-20.6	17.3	43.8	64.7	82.4	97.7
100.	1.0	6.37E+01	-153.5	-88.5	-65.7	-25.7	13.3	40.0	60.9	78.3	93.3
110.	1.4	6.99E+01	-169.7	-99.3	-75.1	-33.0	7.4	34.7	55.8	73.2	88.0
120.	2.0	7.68E+01	-189.0	-112.8	-86.9	-42.5	-.3	27.8	49.4	66.9	81.8
130.	2.7	8.46E+01	-211.2	-128.5	-101.0	-54.0	-9.8	19.4	41.6	59.7	74.8
140.	3.6	9.34E+01	-236.3	-146.5	-117.2	-67.5	-21.1	9.4	32.5	51.2	66.8
150.	4.8	1.03E+02	-264.1	-166.6	-135.4	-83.0	-34.4	-2.3	21.9	41.4	57.7
160.	6.2	1.15E+02	-294.6	-188.7	-155.7	-100.7	-49.7	-16.0	9.6	30.2	47.4
170.	7.9	1.29E+02	-327.7	-212.7	-178.0	-120.6	-67.4	-31.9	-4.8	17.2	35.6
180.	10.0	1.44E+02	-363.4	-238.4	-202.1	-142.9	-87.6	-50.2	-21.4	2.1	22.0
190.	12.5	1.63E+02	-401.7	-265.7	-228.1	-167.6	-110.6	-71.4	-40.7	-15.3	6.4
200.	15.5	1.86E+02	-442.5	-294.3	-255.9	-195.0	-137.0	-96.0	-63.2	-35.5	-11.7

TABLE VIII: SPECIFIC HEAT CAPACITY OF AQUEOUS SODIUM SULFATE SOLUTIONS (JOULE/G DEG)

T (°C)	P (BAR)	D-H SLOPE	CP WATER	MOLALITY .050	.100	.250	.500	.750	1.000	1.250	1.500
25.	1.0	3.28E+01	4.179	4.142	4.108	4.016	3.889	3.786	3.701	3.628	3.565
30.	1.0	3.43E+01	4.178	4.142	4.109	4.019	3.893	3.789	3.702	3.628	3.563
40.	1.0	3.75E+01	4.178	4.144	4.112	4.024	3.901	3.797	3.709	3.633	3.568
50.	1.0	4.09E+01	4.180	4.147	4.115	4.030	3.908	3.804	3.716	3.640	3.574
60.	1.0	4.46E+01	4.184	4.151	4.120	4.035	3.914	3.811	3.722	3.645	3.578
70.	1.0	4.87E+01	4.189	4.156	4.125	4.041	3.920	3.817	3.728	3.650	3.581
80.	1.0	5.32E+01	4.196	4.163	4.132	4.048	3.927	3.823	3.733	3.654	3.584
90.	1.0	5.82E+01	4.205	4.171	4.140	4.056	3.934	3.830	3.739	3.658	3.587
100.	1.0	6.37E+01	4.217	4.183	4.152	4.066	3.944	3.838	3.746	3.664	3.592
110.	1.4	6.99E+01	4.232	4.197	4.165	4.079	3.955	3.848	3.754	3.672	3.597
120.	2.0	7.68E+01	4.249	4.213	4.181	4.093	3.967	3.859	3.764	3.679	3.604
130.	2.7	8.46E+01	4.268	4.231	4.198	4.108	3.980	3.870	3.773	3.687	3.610
140.	3.6	9.34E+01	4.288	4.251	4.217	4.125	3.994	3.882	3.784	3.696	3.618
150.	4.8	1.03E+02	4.312	4.273	4.238	4.144	4.010	3.895	3.795	3.706	3.626
160.	6.2	1.15E+02	4.339	4.299	4.262	4.165	4.028	3.910	3.807	3.716	3.635
170.	7.9	1.29E+02	4.369	4.327	4.290	4.190	4.048	3.927	3.821	3.728	3.645
180.	10.0	1.44E+02	4.403	4.360	4.322	4.218	4.070	3.945	3.837	3.742	3.657
190.	12.5	1.63E+02	4.443	4.399	4.358	4.250	4.097	3.967	3.855	3.757	3.671
200.	15.5	1.86E+02	4.489	4.443	4.401	4.288	4.127	3.992	3.875	3.774	3.686

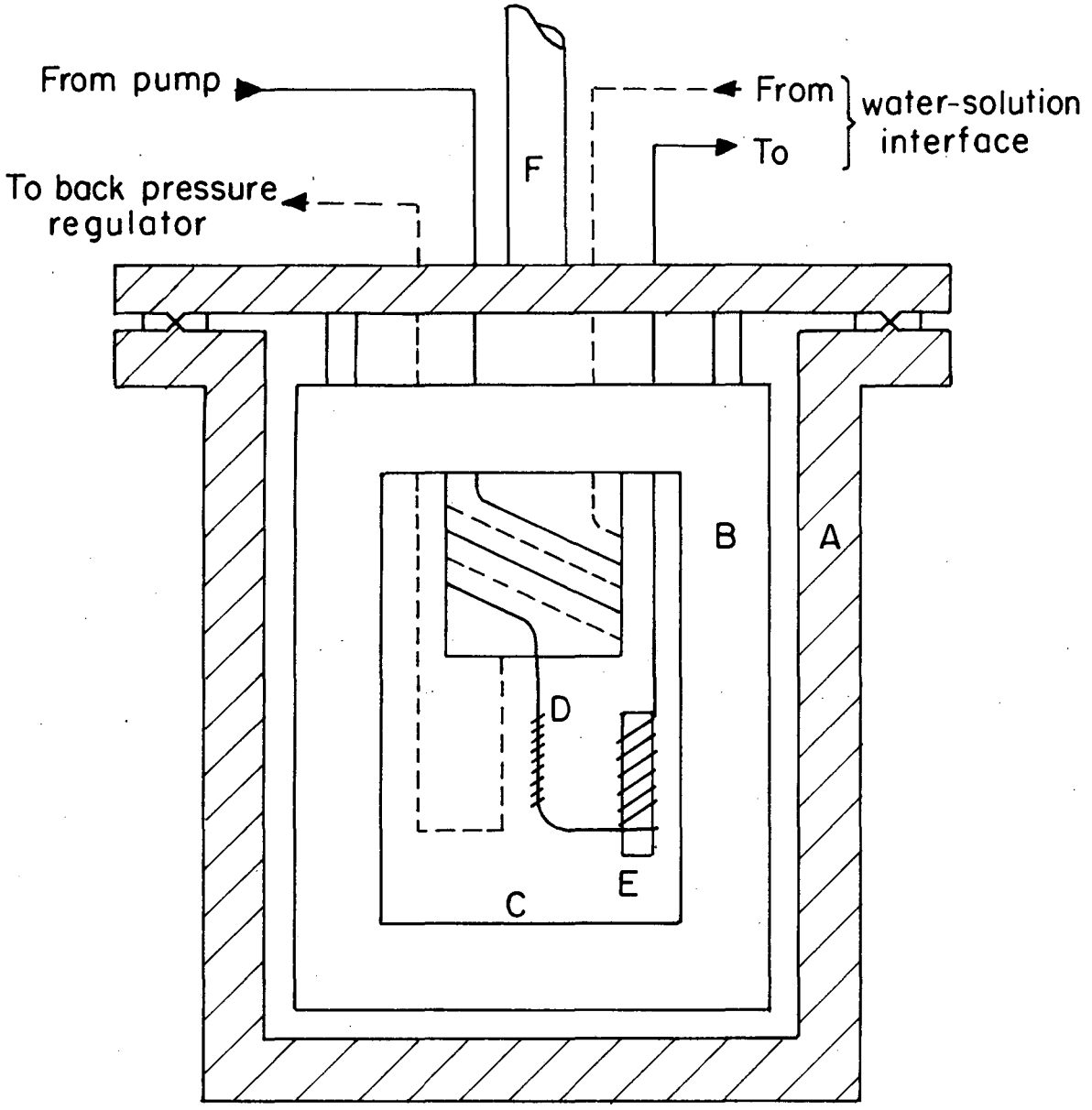
From pump
To back pressure regulator
F
From
To
water-solution interface
B
A
D
E
C
XBL 812-5165

Figure 1

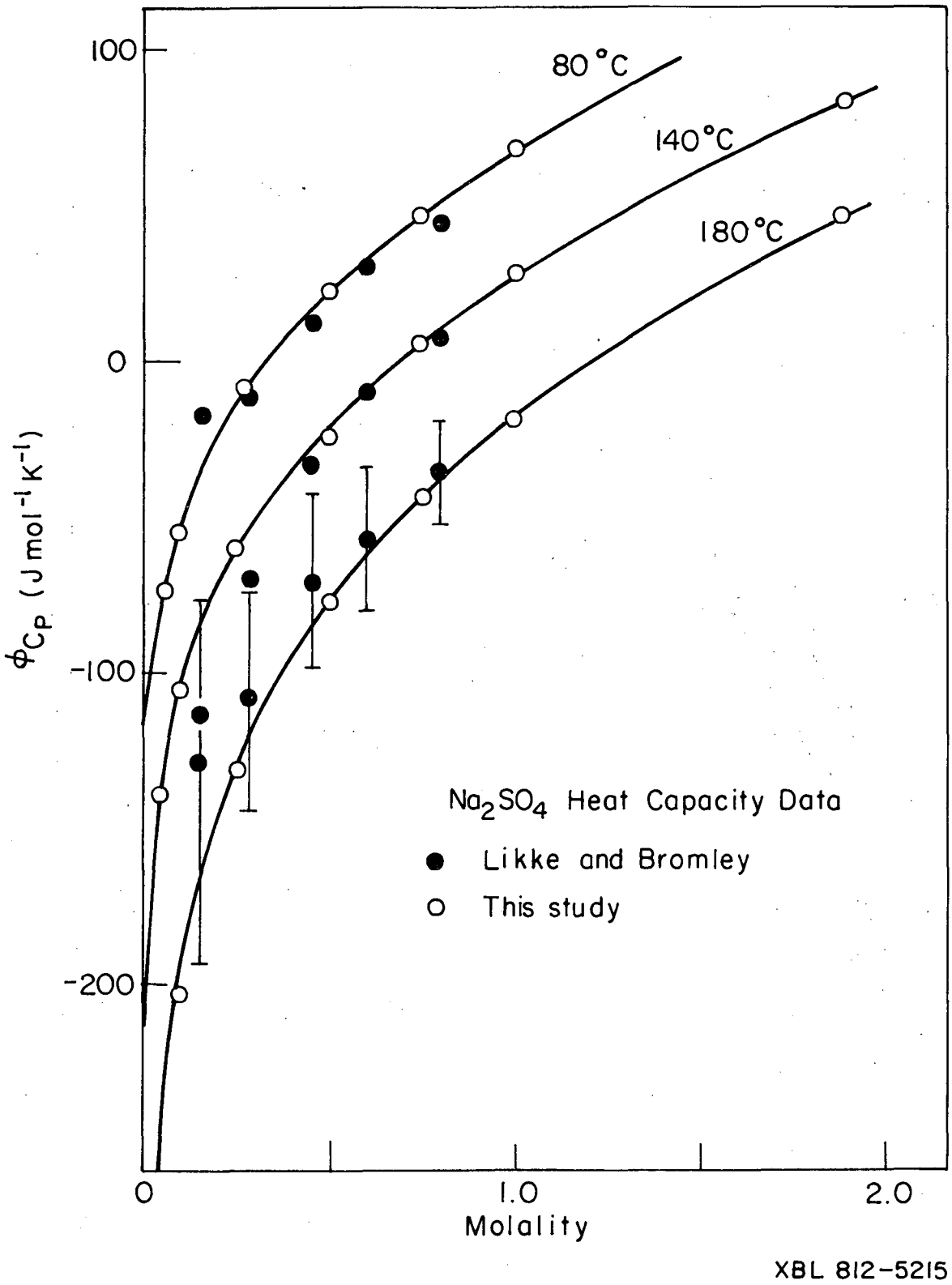
100
0
-100
-200
ϕ_{C_P} (J mol^{-1} K^{-1})
80 °C
140°C
180°C
Na_2SO_4 Heat Capacity Data
Likke and Bromley
This study
0
1.0
2.0
Molality
XBL 812-5215

Figure 2

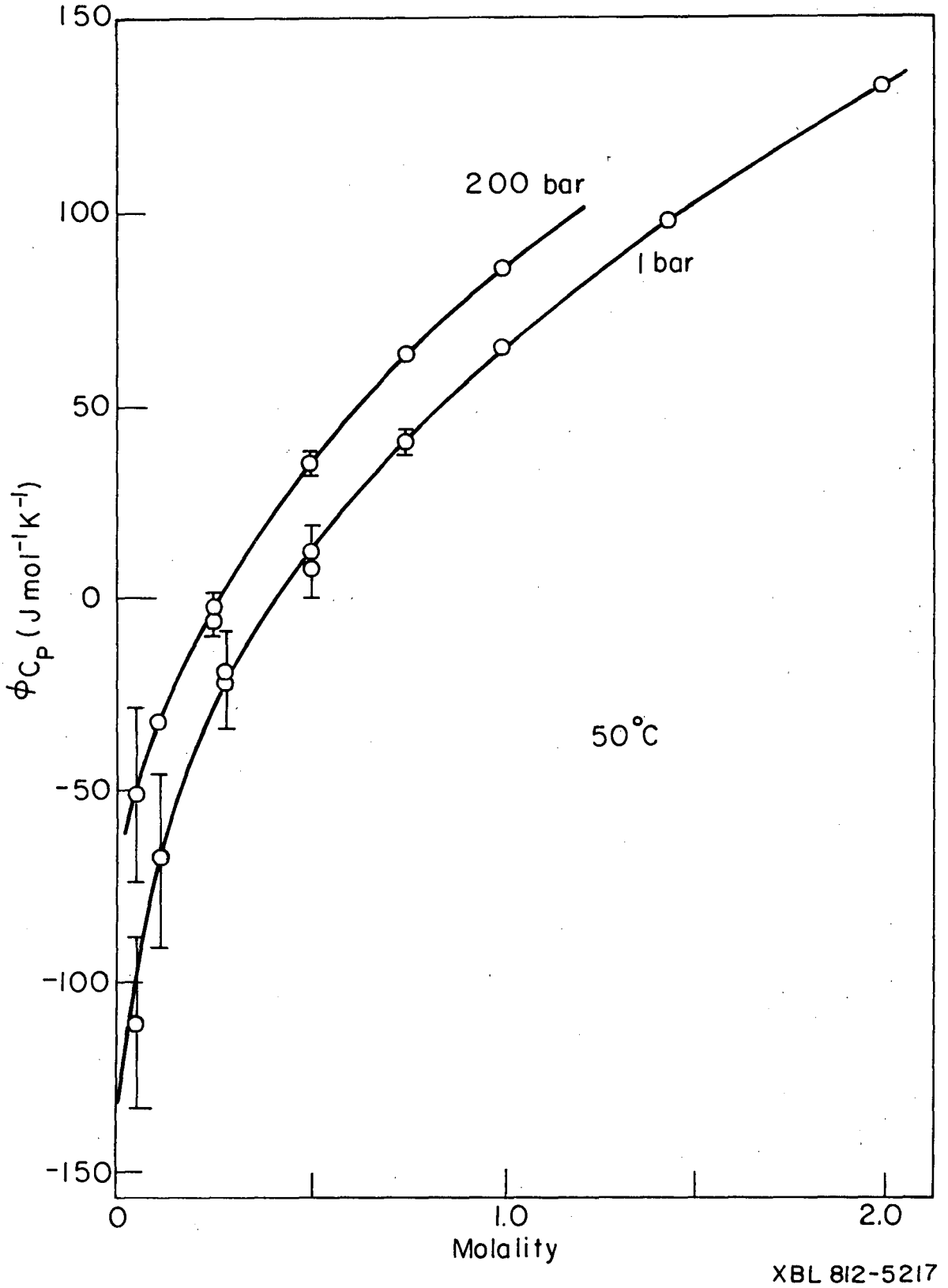
150
100
50
0
-50
-100
-150
ϕC_p (J mol^{-1}K^{-1})
200 bar
1 bar
50°C
0
1.0
2.0
Molality
XBL 812-5217

Figure 3

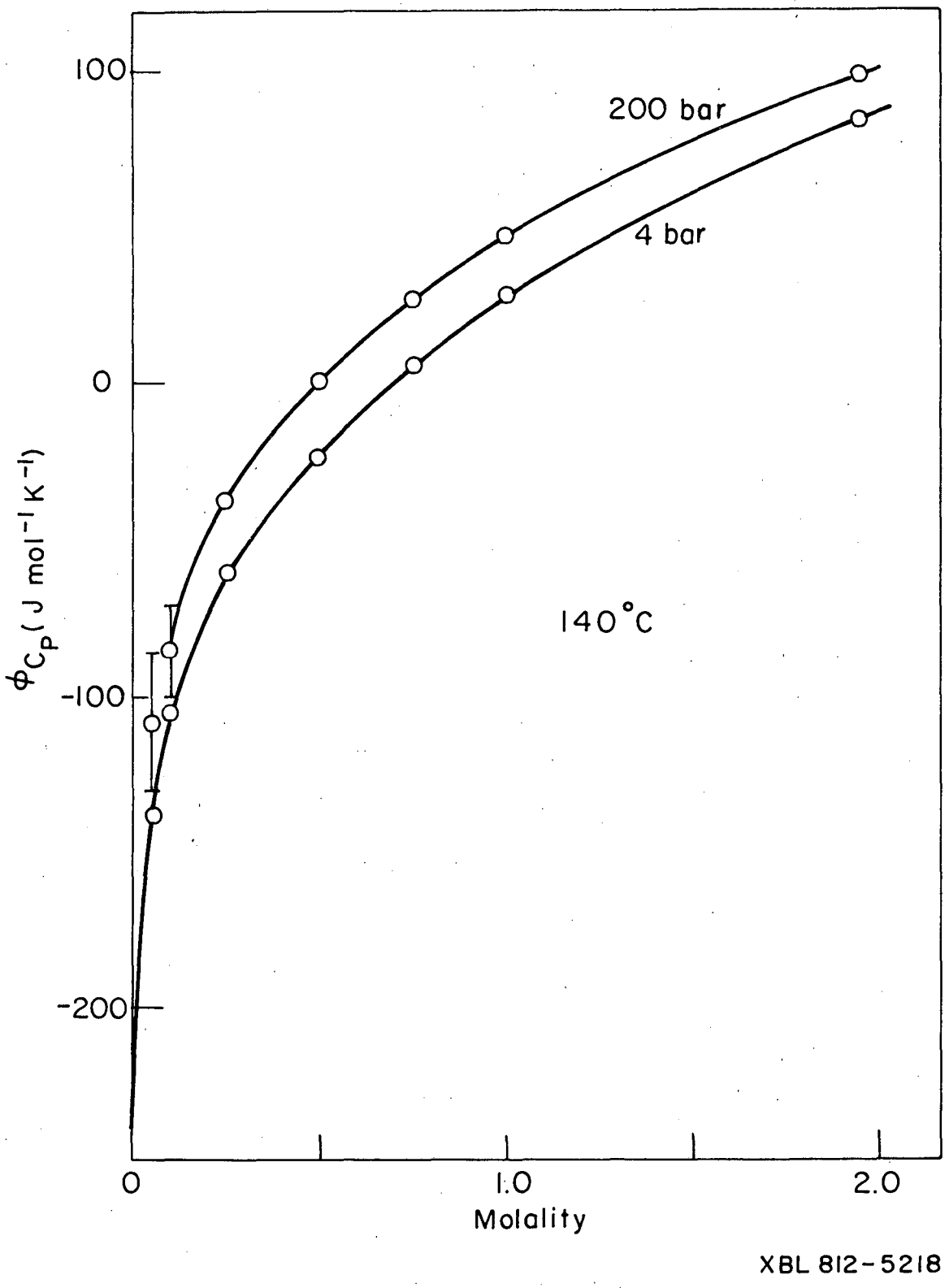
100
0
-100
-200
Φ_{C_P} (J mol^{-1} K^{-1})
200 bar
4 bar
140°C
0
1.0
2.0
Molality
XBL 812-5218

Figure 4

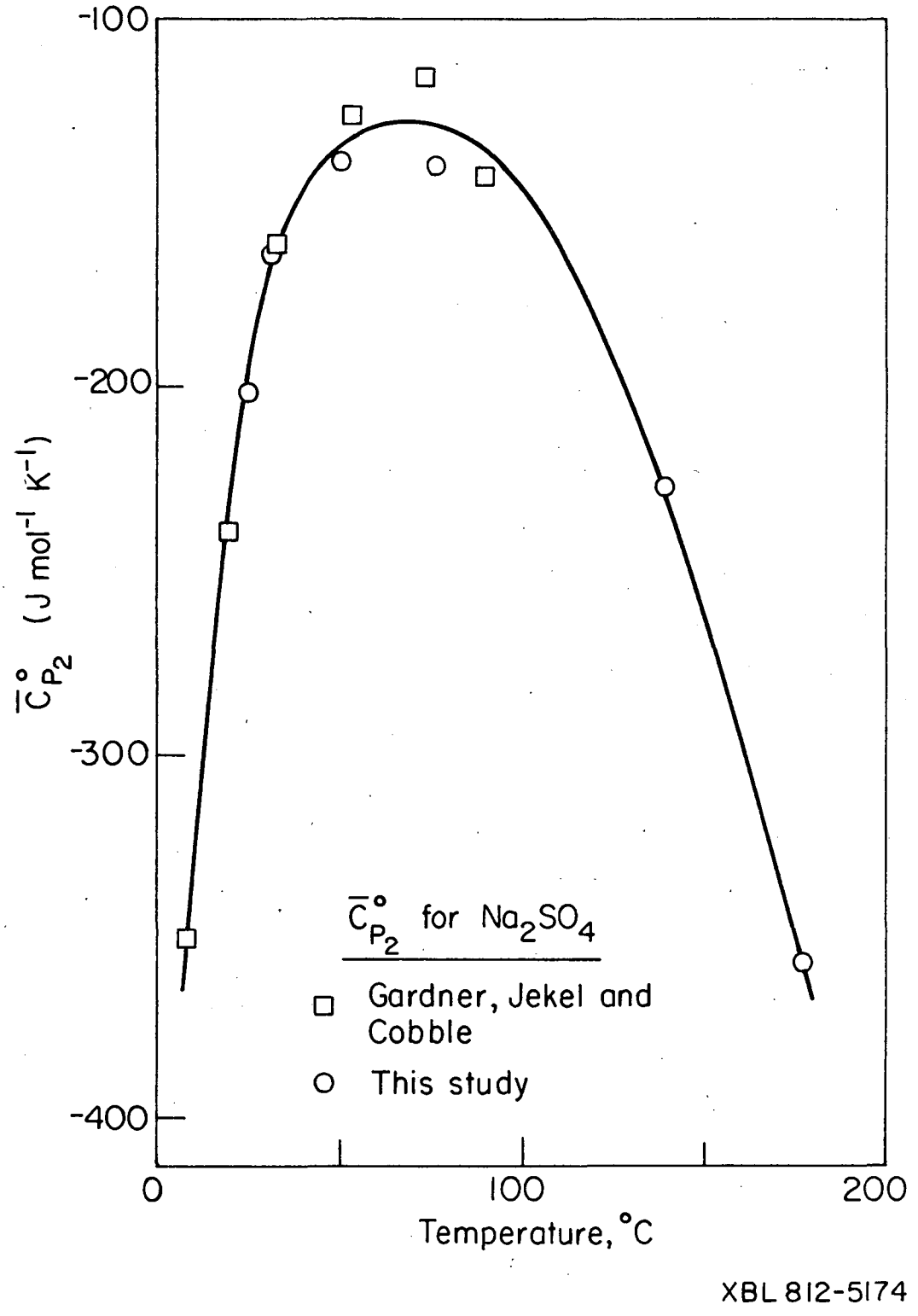
-100
-200
-300
-400
$\bar{C}^{\circ}_{P_2}$ (J mol^{-1} K^{-1})
$\bar{C}^{\circ}_{P_2}$ for Na_2SO_4
Gardner, Jekel and Cobble
This study
0
100
200
Temperature, °C
XBL 812-5174

Figure 5

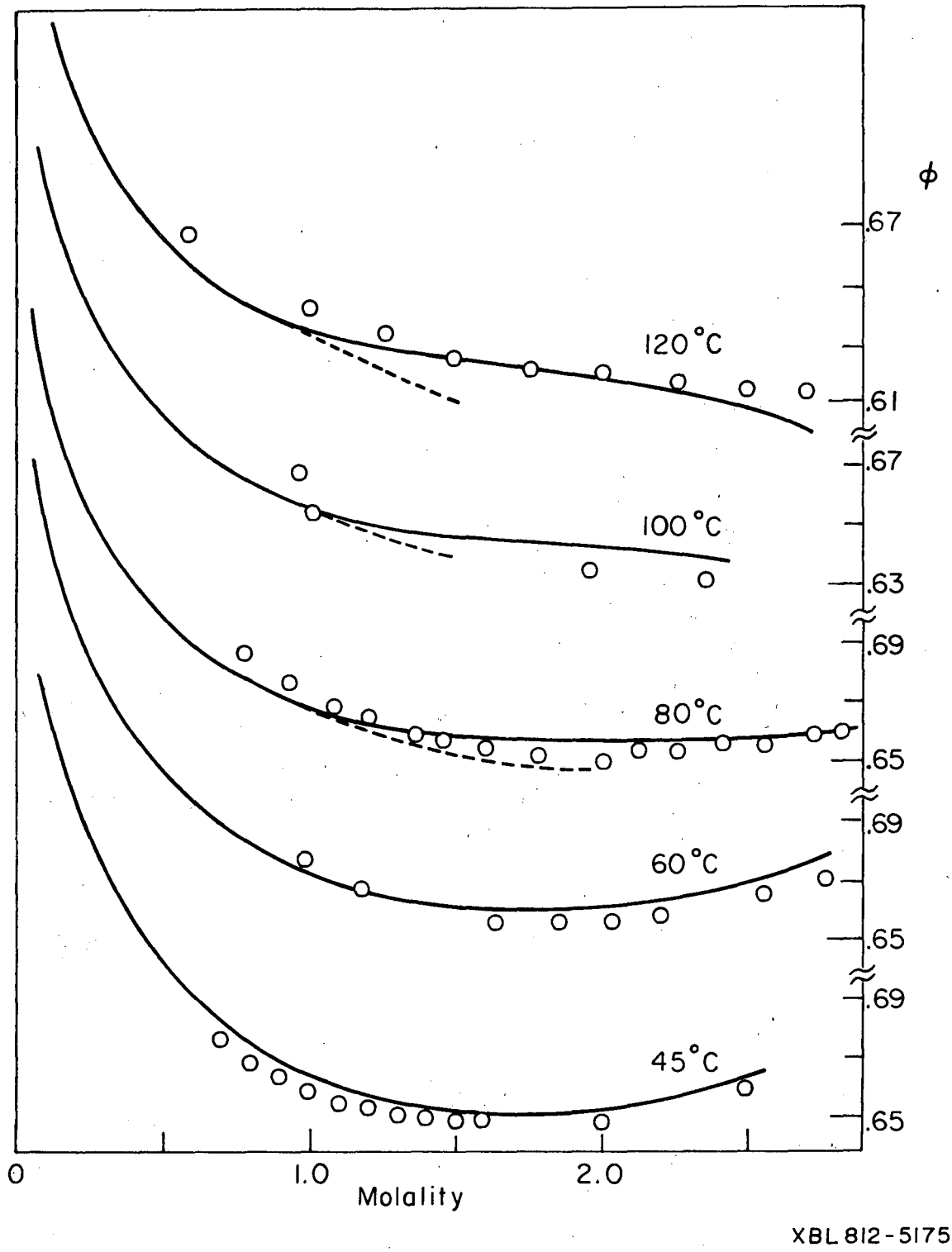
φ
.67
120°C
.61
.67
100°C
.63
.69
80°C
.65
.69
60°C
.65
.69
45°C
.65
0
1.0
2.0
Molality
XBL 812-5175

Figure 6

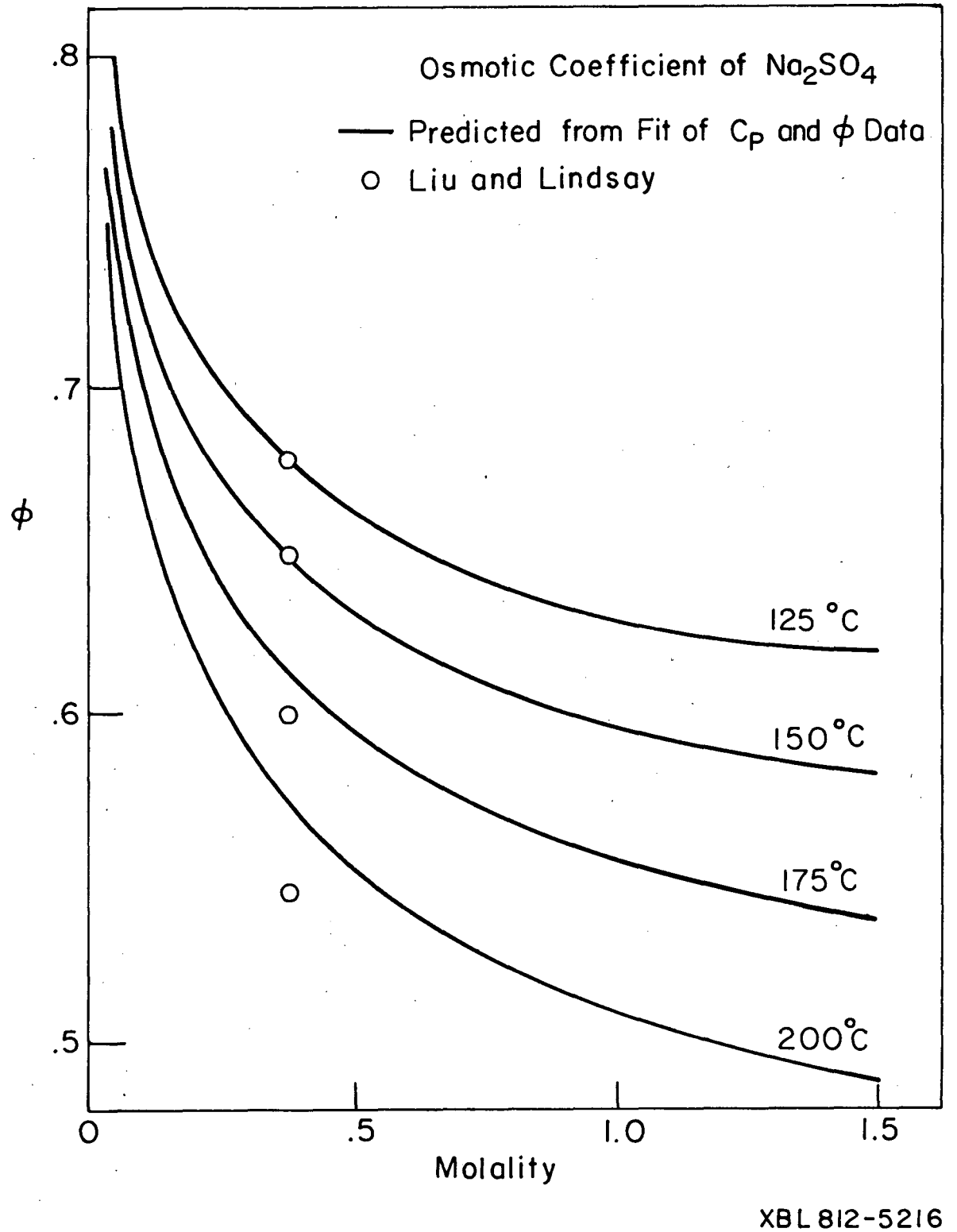
Osmotic Coefficient of Na_2SO_4
Predicted from Fit of C_P and ϕ Data
Liu and Lindsay
125 °C
150 °C
175 °C
200 °C
.8
.7
.6
.5
ϕ
0
.5
1.0
1.5
Molality
XBL 812-5216

Figure 7

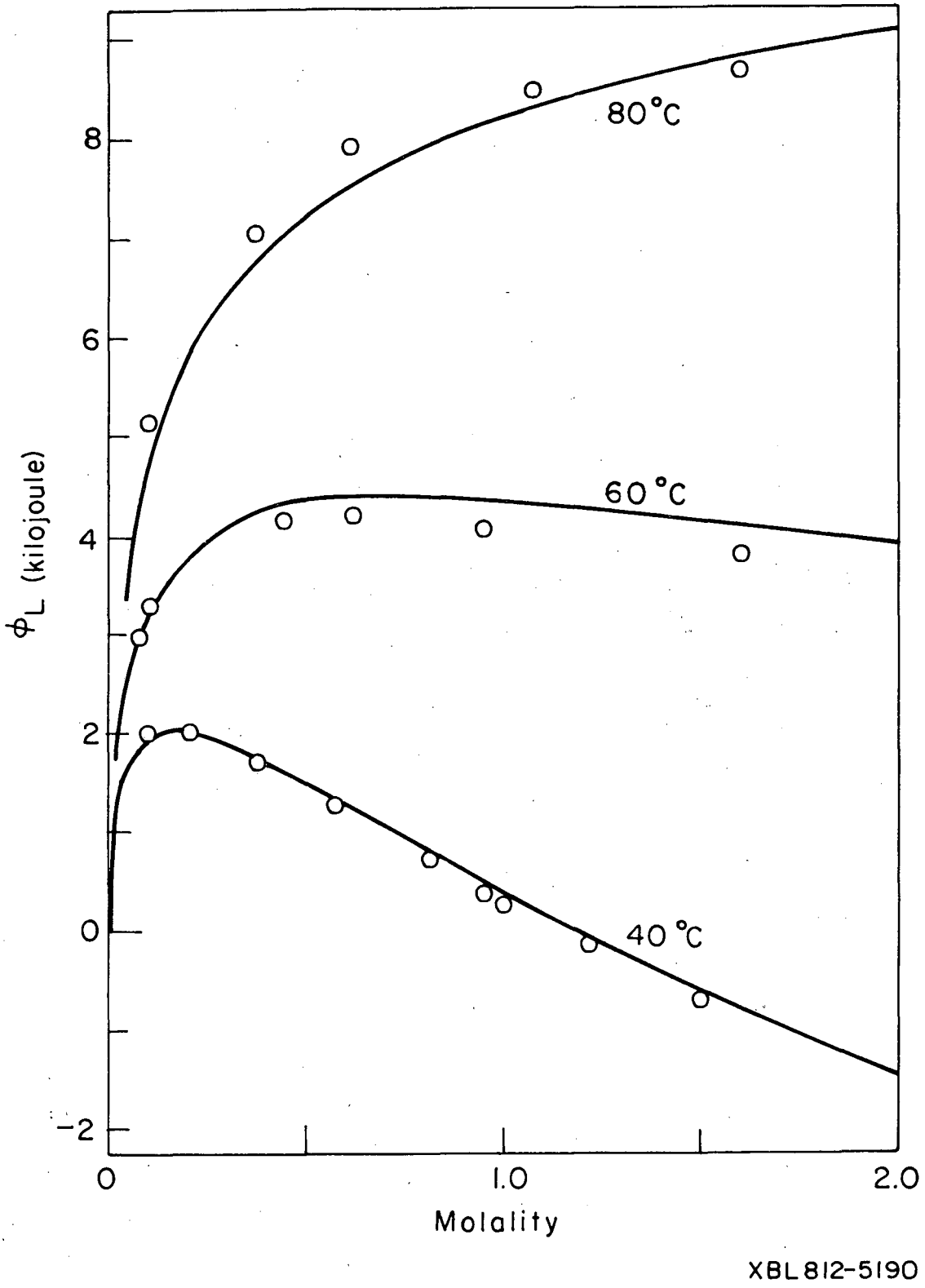
80°C
60°C
40°C
8
6
4
2
0
-2
ϕ_L (kilojoule)
0
1.0
2.0
Molality
XBL 812-5190

Figure 8

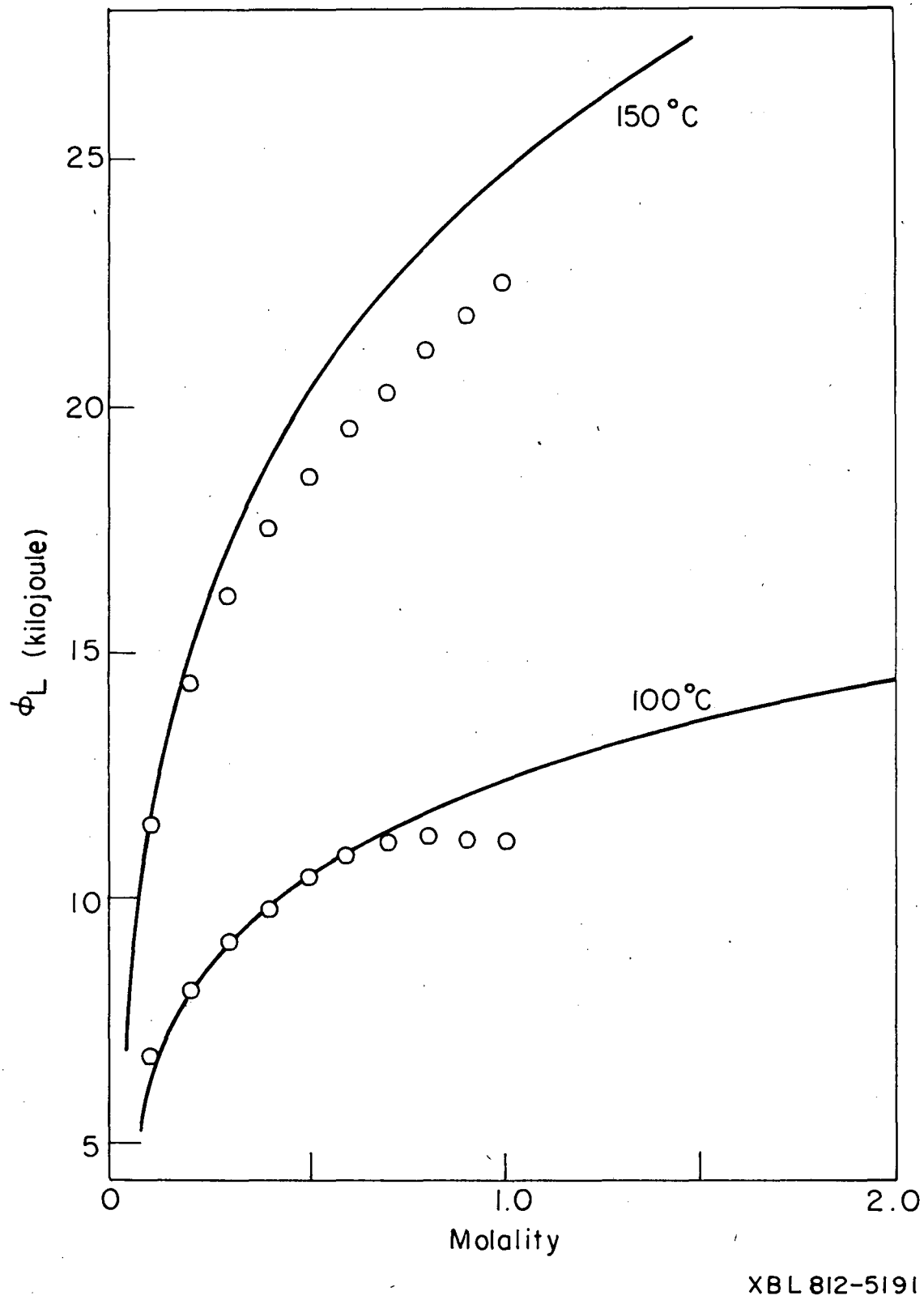
150 °C
100°C
25
20
15
10
5
ϕ_L (kilojoule)
0
1.0
2.0
Molality
XBL 812-5191

Figure 9

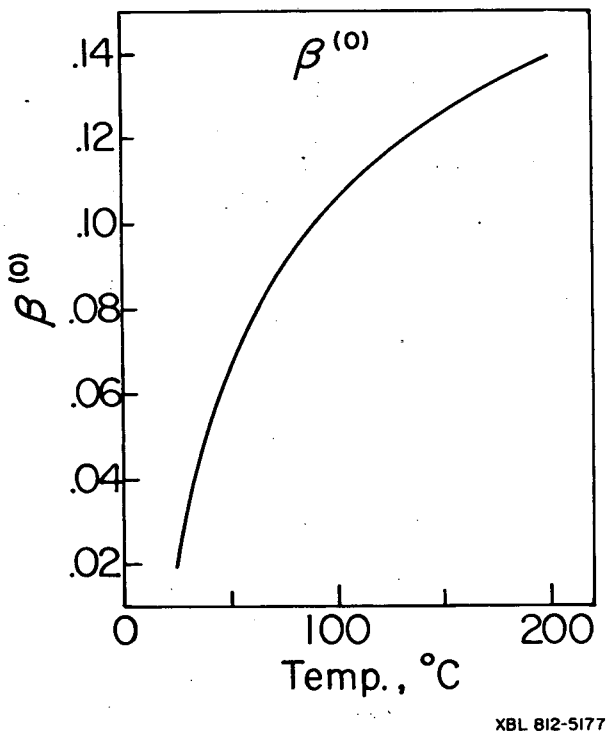
$\beta^{(0)}$
.14
.12
.10
.08
.06
.04
.02
$\beta^{(0)}$
0
100
200
Temp., °C
XBL 812-5177

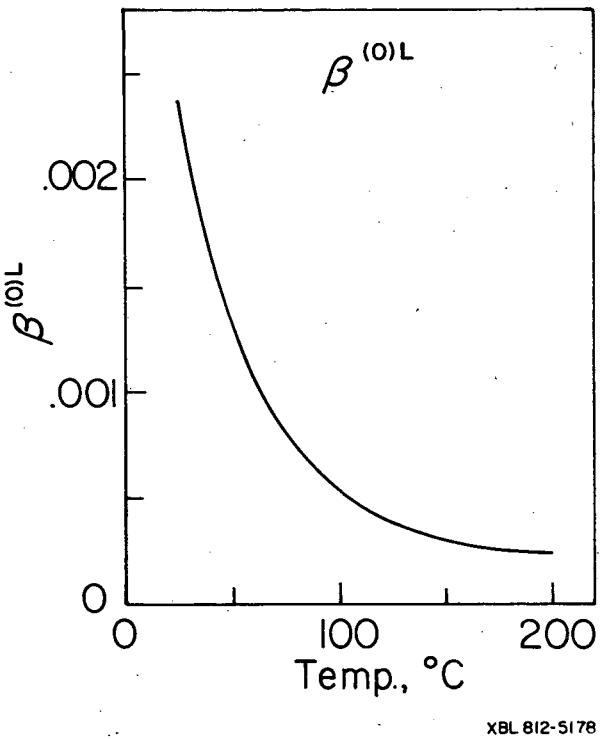
$\beta^{(0)L}$
.002
.001
0
$\beta^{(0)L}$
0
100
200
Temp., °C
XBL 812-5178

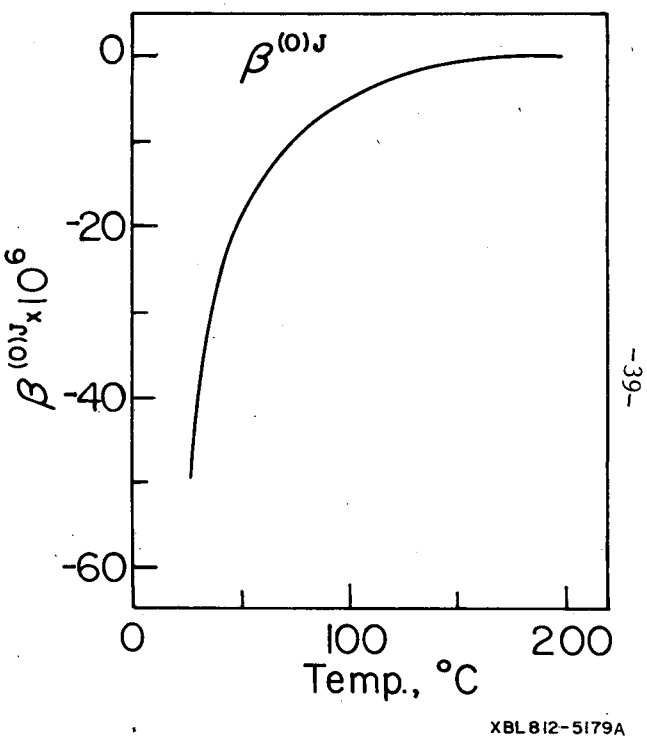
$\beta^{(0)J}$
0
-20
-40
-60
$\beta^{(0)J} \times 10^6$
0
100
200
Temp., °C
XBL 812-5179A

Figure 10

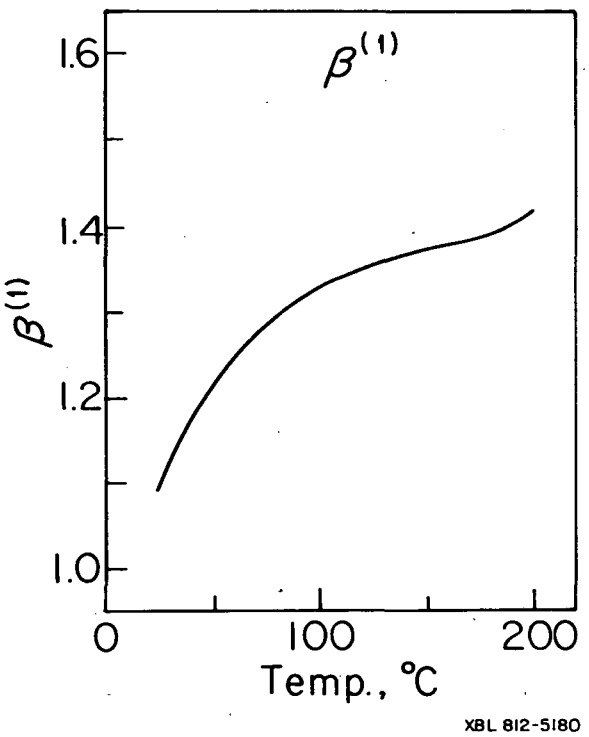
$\beta^{(1)}$
1.6
1.4
1.2
1.0
$\beta^{(1)}$
0
100
200
Temp., °C
XBL 812-5180

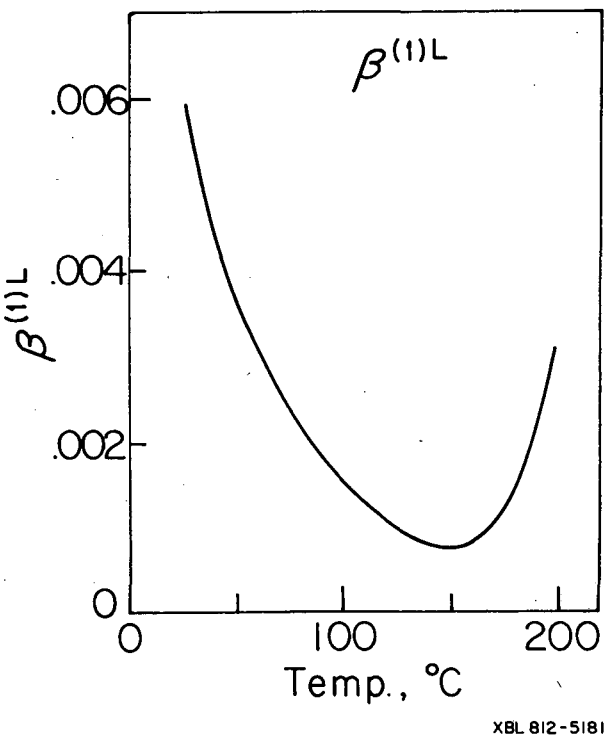
$\beta^{(1)L}$
.006
.004
.002
0
$\beta^{(1)L}$
0
100
200
Temp., °C
XBL 812-5181

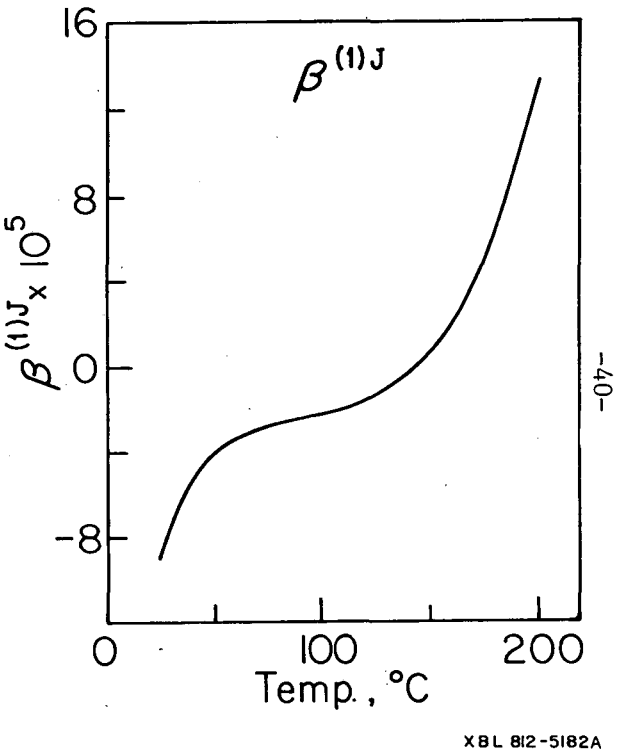
$\beta^{(1)J}$
16
8
0
-8
$\beta^{(1)J} \times 10^5$
0
100
200
Temp., °C
XBL 812-5182A

Figure 11

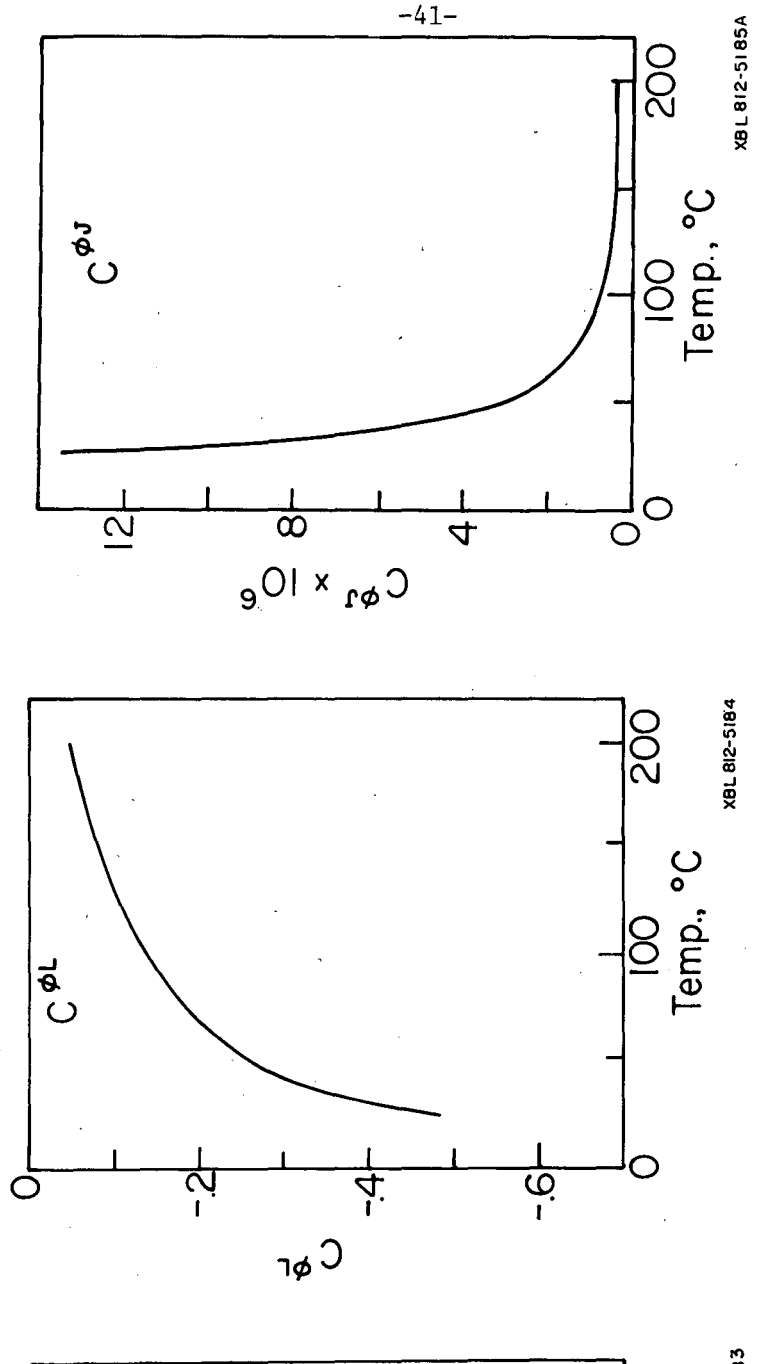
$C^{\phi J} \times 10^6$
12
8
4
0
$C^{\phi J}$
0
100
200
Temp., °C
XBL 812-5185A
$C^{\phi L}$
0
-2
-4
-6
$C^{\phi L}$
$C^{\phi L}$
0
100
200
Temp., °C
XBL 812-5184
C^{ϕ}
0
-.01
-.02
C^{ϕ}
C^{ϕ}
0
100
200
Temp., °C
XBL 812-5183

Figure 12

TECHNICAL INFORMATION DEPARTMENT
LAWRENCE BERKELEY LABORATORY
UNIVERSITY OF CALIFORNIA
BERKELEY, CALIFORNIA 94720